Vol. 4. No. 3. 2021

Contents available at:

www.crdeepjournal.org

International Journal of Research in Engineering & Management (ISSN: 2456-1029)(SJIF: 2.228)

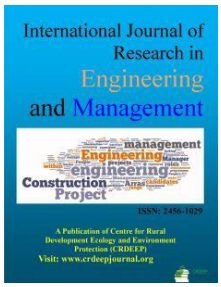

Full Length Research Paper

Numerical Evaluation of Mono-symmetric Steel-concrete Composite section provided with Angle and Channel Shear Connectors.

Ahmed Kamar[1, a], Mahmoud Lasheen[2], Amr Shaat[3], Amr zaher[4], Ayman Khalil[5]

[1] *Ph.D. student at Department of Structural Engineering, Ain Shams University, Cairo, Egypt.*

[2] *Concrete Construction Research Institute, Housing and Building National Research Center, Cairo, Egypt.*

[3,4,5] *Department of Structural Engineering, Ain Shams University, Cairo, Egypt.*

[a] *Department of Construction and Building, Faculty of Eng., October 6 University, Giza, Egypt.*

ARTICLE INFORMATION

Corresponding Author:
Ahmed Kamar

Article history:
Received:07-03-2021
Accepted: 10-03-2021
Published: 12-03-2021

Key words:
Finite element, experimental, mono-symmetric composite beam, effective width, shape of shear connectors,

ABSTRACT

In this paper, a nonlinear finite element model (FEM) was developed using ABAQUS 6.14 to determine the behaviour of mono-symmetric steel-concrete composite (SCC) beams provided with angle or channel shear connectors. Also, validation of the results of the FEM against the experimental results is discussed in this paper. Moreover, the FEM will be used to calculate the effective width of the concrete slab against the slenderness ratio (L/rs) of the steel beam, the type of the shear connector placed at the top flange of the steel beam and the existence of upper steel reinforcement mesh and comparing the results with the calculation of the effective width in the universal codes (i.e., AISC 360-15, CSA S16-14 and the Eurocode 4; CEN 2004). Also, the effective concrete slab width for each SCC beam will be compared according to the equation developed by Lasheen et al. In this respect, ten(SCC) beams were modeled to study the effect of the steel section and shapes of the shear connector on the SCC beams' behaviour and compare the results with the experimental results. The results of this study showed that the average ratio between the FEM and experimental results for ultimate loads is 99.75%. Therefore, the finite element models can be used with confidence to extend the experimental program and investigate a wider range of parameters. Also, the results of the FEM Proved that the effective slab width for beams decreases as the slenderness ratio of the steel section increases.

Introduction

Composite steel-concrete solutions represent a widely used form of construction applications. The SCC beams formed by two dissimilar materials attached together to act as one unit. The SCC beams have significant advantages in terms of their bending resistance and stiffness, allowing maximum use of the material strengths of both steel and concrete and taking advantage of the lightweight and fast construction features.In SCC, the use of a mono-symmetric steel section is more economical than the use of a double-symmetric section of steel. This is attributed to the presence of the concrete slab in the compression zone of the SCC beams.

The performance of steel-concrete composite (SCC) beams depends significantly on the force transfer mechanism at the interface between the steel beam and concrete [1,2]. Shear connectors are used to reduce the slippage at the steel-concrete interface. The degree of the composite action is an essential principle for the design of composite beams, which significantly affects the composite beam's flexural response. Partial composite action can result in higher slip rates at the interface between the concrete slab and the steel beam, potentially resulting in increased deflection of the SCC beams. In the case of full composite action, the slip rate estimate may also be important [3]. The behaviour of the angle shear connector in SCC Structures was studied. The results showed that the shear resistance and the shear stiffness of the angle connectors show good prediction compared with other connectors [4]. Kamar et al. [5] conducted an experimental study on ten SCC beams to evaluate the behaviour of using a mono-symmetric steel-concrete composite section provided with angle and channel shear connectors.The results showed that the ultimate load capacity of composite beam with angle connectors is 14% lower than the counterpart beam with channel connectors. In addition, it is found that beams provided with channel shear connectors are more likely to be more ductile than that beams provided with angle shear connectors by 39.9%. Simple analytical models are also available

to depict the force transfer mechanism between the concrete slab and steel beam [6-12]. It is important to understand the nonlinear behaviour of the shear connector.

In SCC beams, the concrete slab is subjected to variable compression stresses over its overall width and thickness. The effective slab width is a term used to simplify the calculation of the bending stresses of SCC beams. The distribution of longitudinal compressive stress over the width of the concrete slab is non-uniform with high values above the steel beam,which decreases at the extremities [13]. This is called the "shear lag" phenomenon. The exact calculation of the SCC beams' effective flange width leads to an accurate estimation of the predicted deflection. The effective width calculation in the universal codes (i.e., AISC 360-15 [14] & CSA S16-14 [15]) depends on the span and spacing of the beams between the steel beams. In addition, the concrete slab thickness is negligible. Most recent research in the field of composite beams has introduced different new parameters affecting the effective width of the slab [16-17]. The shape of the shear connector has a slight effect on the effective width of the concrete slab[5]. The slenderness ratio of the steel section is considered one of the most critical parameters that affect the value of the effective slab width [17].

The presence of the upper transverse steelreduces or prevents the appearance of cracks in the upper side concrete slab, which affects the capacity of the composite beams, the slip value between the concrete slab and steel beam and the calculation of the effective width of the slab. However, the codes and specifications neglect the presence of the upper steel reinforcement meshin calculating the capacity of the composite beams.

The thickness of the concrete slab has a negligible effect on the effective concrete slab width. This is due to the equilibrium of force along the steel-concrete composite section, where the upward move in the neutral axis is equal to the slab thickness increase [17]. However, the ultimate load capacity is increasing with increasing the slab thickness. Also, the beams' deflection value is affected by increasing the concrete slab thickness, where increasing the slab thickness is decreasing the deflection. Besides, increasing the slab thickness reduces the slip value. In this respect, a numerical investigation is carried out to evaluate the effective concrete slab width in the mono-symmetrical steel section. The numerical program results and the analysis of the results will be discussed to evaluate the effective concrete slab width in mono-symmetrical steel sections. Also, the effective slab width value extracted from the numerical analysis will be compared with the experimental results and with the calculation of the effective width in the universal codes (i.e., AISC 360-15, CSA S16-14 and the Eurocode 4; CEN 2004[18]). Also, the numerical results will be used to investigate the effect of using the upper reinforced steel mesh on load capacity. The effect of top reinforcementmesh on the effective slab width of a mono-symmetric steelsection will also be discussed in thecurrent study.

Finite element model

Tenspecimens were modelled using ABAQUS 6.14 [19] to simulate the SCC beams that were tested in the experimental program [5], as listed in Table 1. The details of beams are shown in Figures 1 and 2. This numerical model was carried out to verify the FE models against the experimental results in terms of load-deflection, load-slip and load strain responses.

Boundary conditions and load arrangements

Due to the symmetry in the geometry, loading and boundary conditions, one-quarter of the specimen was modelled, asshown in Fig. 1. The coordinate axes X, Y and Z are represented as axes 1, 2 and 3 in the model, respectively. The symmetryplanes are shown in Fig. 1. The external loads have been modelled as equivalent pressure on the top surface of the concrete slab over a contact width of 100 mm x 200mm at load point location to reflect the actual effects of the loading and spreader beams that were used in the experiments.

Element type and mesh

The accuracy of the results depends on the meshing of elements, constitutive material models and boundary conditions. So, these parts are accurately investigated in the proposed FE model. In the current study, the concrete and steel parts of the model are modeling with eight-node brick elements with reduced integration (C3D8R) that have been chosen with a maximum mesh size of 20 mm.The reduced integration avoids the requirement of higher-order solid elements without compromising the reliability of the measured responses. This element takes care of hourglass issues which commonly arise with continuum linear solid elements. A regular structured hexahedral mesh is used. The reinforcement bars were defined using three-dimensional truss elements(T3D2) in linear order. This element was used for all reinforcement types with a maximum mesh size of 20 mm.

Material model

Concrete modeling

ABAQUS 6.14 has the ability to simulation the damage for reinforced concrete elements using either of the three crack models: Smeared crack concrete model, Brittle crack concrete model and concrete damaged plasticity model. The concrete damage plasticity model is used to model the concrete slab in the current research. This model has the ability to represent the complete inelastic behaviour of concrete both in tension and compression, including damage characteristics. The concrete damaged plasticity model assumes that the two major failure mechanisms in concrete are tensile cracking and compressive crushing. In this model, the uniaxial tensile and compressive behaviour is characterized by damaged plasticity. The compressive strength defined in this study for the NWC is 28 MPa. The Young's modulus of the proposed NWC is 24 GPa.The density and Poisson ratio of concretes are considered as 25 kN/m^3 and 0.2, respectively.For defining the strain-softening behaviour for cracked concrete, tension stiffening is used to model the post-failure behaviour for direct tension across cracks. The total strain at which the tensile stress equal zero is taken in many previous studies is 10 times the tensile cracking strain. However, it has been found that this value was not suitable for concrete slabs in SCC beams [20,21]. As mentioned by Liang et al. [22], a total strain of 0.1 is preferably used for reinforced concrete slabs in SCC beams.

Steel modeling

For steel material, the Bi-linear model is used. The properties of the steel sections, shear connectors and steel reinforcement bars are modelled with the same properties as the tested specimens.

The elastic properties of the steel beams were taken equal to 210 GPa for Young's modulus and 0.3 forPoisson's ratio. The yield and ultimate strengths are taken as shown in Table 2.

Steel-concrete interaction

The interaction between the concrete slab and the internal steel reinforcement bars was defined using the truss in solid technique option that was used in ABAQUS 6.14. This technique simulating the concrete slab as the host region by the continuum solid elements while the reinforcement bars simulating as the embedded elements by truss elements.To modeling the contact surface between the concrete slab and channel shear connector and the contact surface between the lower surface of the concrete slab and the upper surface of the steel beam flange, the surface-to-surface contact algorithm was used. The channel shear connector was selected as the master surface, while the concrete slab was selected as the slave surface. Also, the upper steel flange was selected as the master surface, while the concrete slab was selected as the slave surface. The contact property was defined by tangential behaviour to consider the factors of friction and elastic slip and by normal behaviour to consider the factors of penetration and separation. Penalty friction formulation with a coefficient of 0.5 was selected to its tangential behaviour and hard pressure over closure was selected to its normal behaviour. Welded regions, such as the welded lines between the shear connector and steel beam flange, the welded lines between the upper flange, web and the lower flange of steel beam and the welded lines between stiffener and web of steel beam were modelled using tie constraints, where there is no separation at weld positions.

Validation of the finite element model

TheFEM is validated against the ten tested specimens. To verify the FEM, a comparison between the experimental results obtained from tests and those from the FEA was carried out in the following sections. The FEM results, including the mid-span deflection and typical modes of failure for each of the models, are presented. The FEM showed good agreement with the experimental results.

Strength of beams

Table 3 shows the ultimate load capacity obtained from the FEM predictions and the corresponding experimental program results for the specimens. Also, Table 3 gives the ratio between the FEM and the experimental program results for the ultimate loads values. The results show that the average ratio between the FEM and the experimental results for ultimate loads is 99.75% with a standard deviation of 0.45%, as shown in Table 3.These small deviation values indicate the reliability of the FEM results. The ultimate loads obtained from the FEM appear the load levels at which the model failed to reach convergence, which means either the steel or the concrete strain reached its ultimate value, or a stability failure occurred. Also, Table 3 shows that the maximum difference between the FEM and experimental ultimate load is in the range of 1%.

Load-deflection behaviour

For all specimens, the FEM and experimental results were be compared in terms of load-deflection behaviour, as shown in Fig. 4. According to the load-deflection curves, it is noted that FEM results show good agreement with the experimental results. The FEM is considered reliable in predicting the deflection values until failure. Table 3 lists the maximum deflection values obtained at the same load level for FEM results and experimental tests. The results show that the difference between the FEM and experimental results for ultimate deflection is in the range of 0.5% with a standard deviation of 0.87% for all specimens. Also, Table 3 shows the elastic stiffness values for both the tested specimens and FE models. It can be noted that the average ratio between the experimental and FEM in terms of elastic stiffness is in the range of 4% with a standard deviation of 8.23%.

Failure modes

All FEM showed the same failure mode as the experimental specimens. Additionally, the FEM followed the same sequence of failure as the experimental specimens. The failure signs included the initiation of yielding at the steel section, initiation of transverse, longitudinal cracks in the concrete slab and horizontal slip between the concrete slab and the steel beam. The typical failure sequence of all specimens is shown in Fig. 5.These figures are used to compare the FEM and experimental cracking schemes for the concrete slab.

The figures show the typical tension or compression damage of concrete slab reached by the FEM and their counterpart experimental failure modes for all beams. The figures also display the compression and tension stresses in both the z-z and x-x directions, respectively, that caused the crack to the concrete slab. The FEM results showed that no damage in the concrete slab for all specimens due to the maximum capacity of the concrete slab is almost close to the capacity of the shear connectors between the point of the maximum positive moment and the point of zero moments, where the showed stresses at the concrete slab did not reach the maximum compressive concrete stresses.

These results comply with the experimental modes of failure. Fig. 5(a) shows the initiation of longitudinal tension crack at the upper concrete slab face at the mid concrete slab for beams without the upper steel reinforcement mesh, which means that the concrete slab reached the cracking tensile stresses at the upper concrete slab face in the x-direction.

There are no longitudinal cracks on the upper side of the concrete slab for beams with the upper steel reinforcement mesh. Moreover, the FE model showed tension crack at the underside of the concrete slab for all beams, as shown in Fig. 5(b). On the other hand, the model did not show tension damage at the underside of the concrete slab for all beams, as was observed in the experiments. Hence, the FEM can detect all concrete slab failure modes either in the compression side or the tension side. Also, the behaviour of the slip of the steel beam interface for all beams in the numerical model shown the same trend in the experimental specimens, as shown in Fig. 5(c).

Model validity

According to the presented validation results, the models show a good agreement with the experimental results. So, the FE models can be used with confidence to expand the experimental program and investigate a wider range of parameters.

Table 1. Details of Test Specimens.

Beam ID	Total Length (mm)	Span, L (mm)	Slab width, Bs(mm)	slab thickness, ts(mm)	Connector shape	h w (mm)	t w (mm)	t f (mm)	b L (mm)	b u (mm)	L/d	L/rs	Upper transverse steel
B1	5000	4800	1200	80	UPN 60	260	8	12	200	100	13.18	42.2	Without
B2					Angle 60								
B3				140	UPN 60						11.32		
B4				120	Angle 60						11.88		
B5				140	UPN 60						11.32		With 5Ø10/m
B6				120	Angle 60						11.88		
B7				80	UPN 60	200		10	160	80	16	55.4	Without
B8					Angle 60								
B9					UPN 60	150	6		120	60	19.2	70.9	
B10					Angle 60								

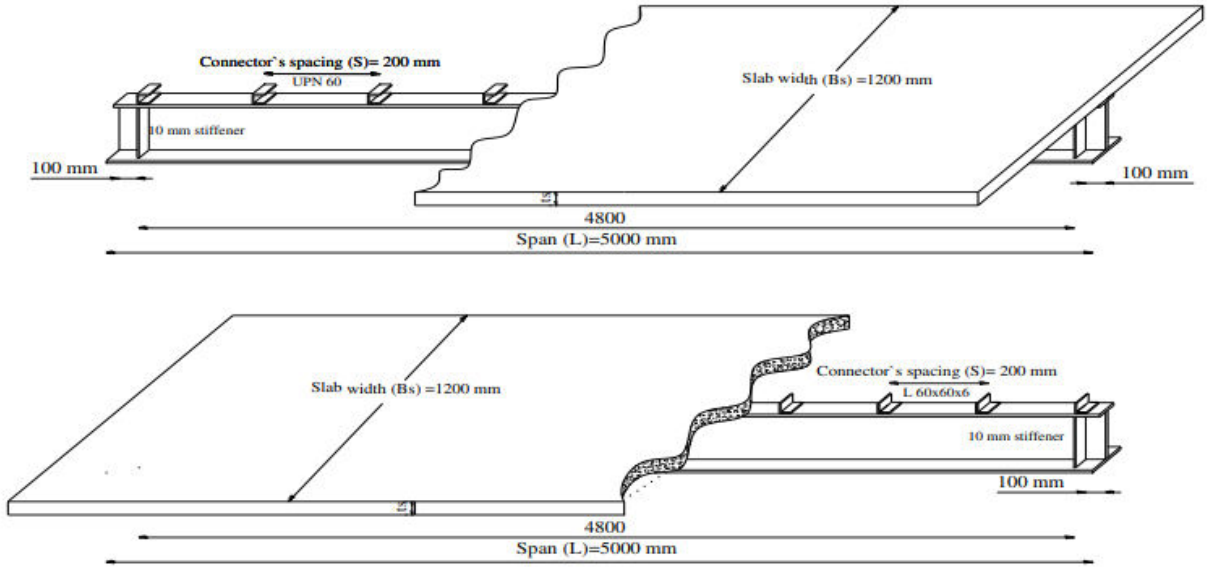

Fig. 1. Details of test specimens.

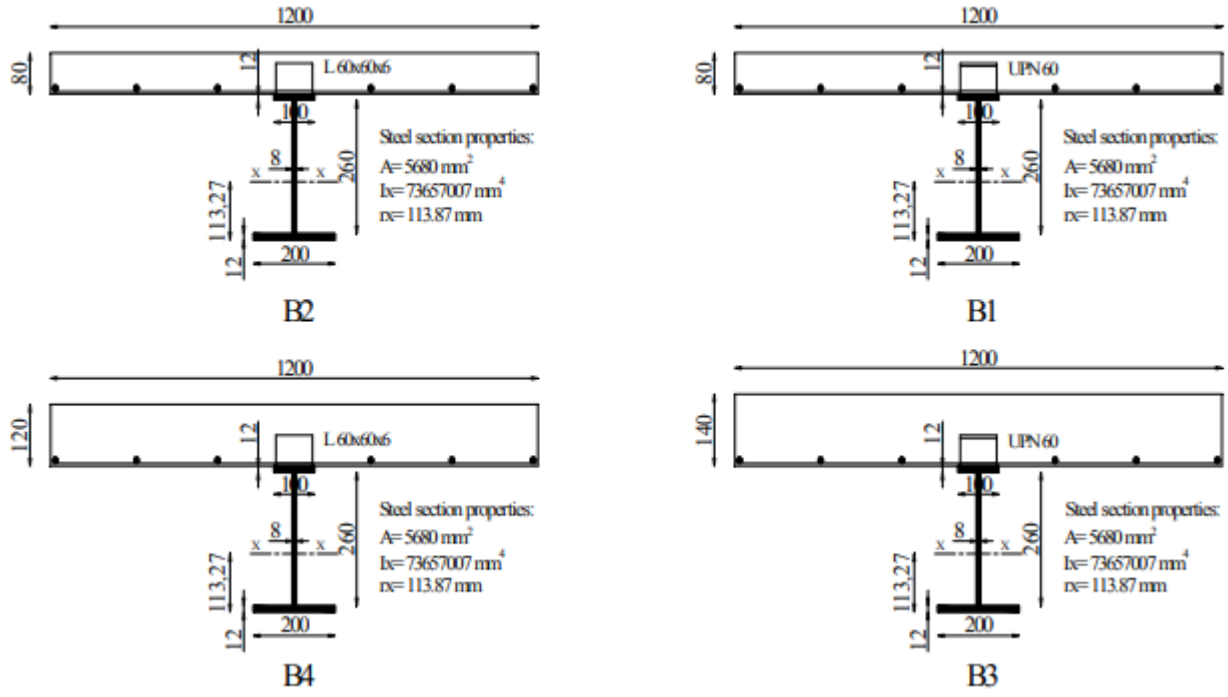

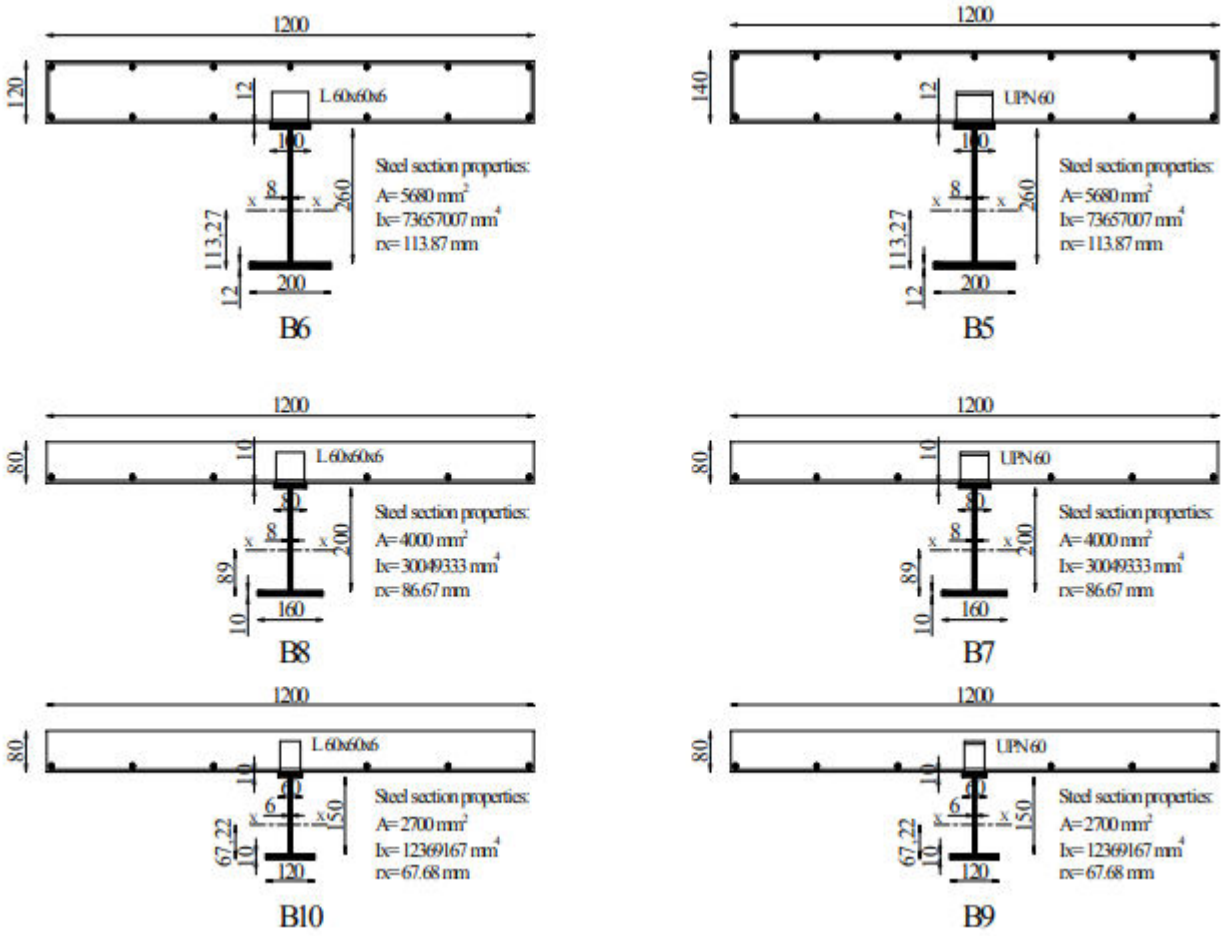

Fig. 2. Dimensions of test specimens.

Table 2. Mechanical properties of steel plates and steel reinforcement.

Steel Section	Average Yield Stress, fy (MPa)	Average Ultimate Stress, fu (MPa)	Average Young's Modulus, E (GPa)	Average Elongation/ Shortening at ultimate %
Plate 6 mm	275	470	210	27
Plate 8 mm	290	470	210	28.3
Plate 10 mm	320	550	210	21.97
Plate 12 mm	360	550	210	21
Diameter 8 mm	350	435	200	13.6
Diameter 10 mm	490	570	200	14.1

Table 3. Comparison between ultimate loads for FEM and Experiments.

BEAM	Failure Load (P_u) KN		Stiffness (P_y/δ_y)at the Elastic Stage(kN/mm)		Deflection at P_u (mm) δ_u		% (F.E./EXP.)		
	EXP.	F.E.	EXP.	F.E.	EXP.	F.E.	P_u	(P_y/δ_y)	δ_u
B1	457.67	455.95	12.93	12.38	64.38	64.87	99.62	95.75	100.76
B2	459.93	457.65	12.64	14.16	67.04	66.59	99.50	112.03	99.33
B3	581.3	576.82	21.74	25.88	57.15	57.24	99.23	119.04	100.16

B4	549.63	548.64	20.37	20.24	55.21	55.52	99.82	99.36	100.56
B5	624.62	625.41	24.33	26.53	69.68	69.03	100.13	109.04	99.07
B6	565.16	565.58	23.03	24.10	48.66	49.48	100.07	104.65	101.69
B7	220.29	220.77	6.61	6.77	74.27	75.57	100.22	102.42	101.75
B8	209.11	208.30	4.52	4.74	77.74	77.86	99.61	104.87	100.15
B9	131.64	132.09	2.78	2.93	136.84	137.59	100.34	105.40	100.55
B10	117.69	116.44	2.87	2.58	79.02	79.12	98.94	89.90	100.13
						average	99.75	104.24	100.41
						Standard deviation	0.45	8.23	0.87

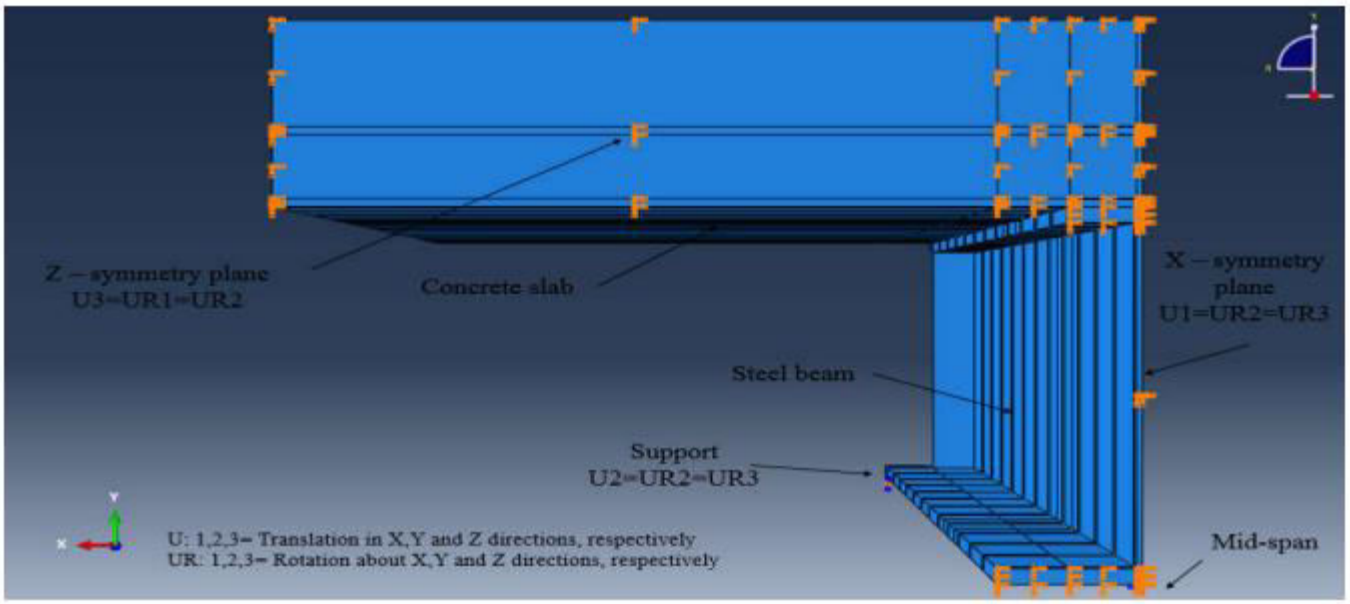

Fig. 3. Boundary conditions for one quarter of SCC beam.

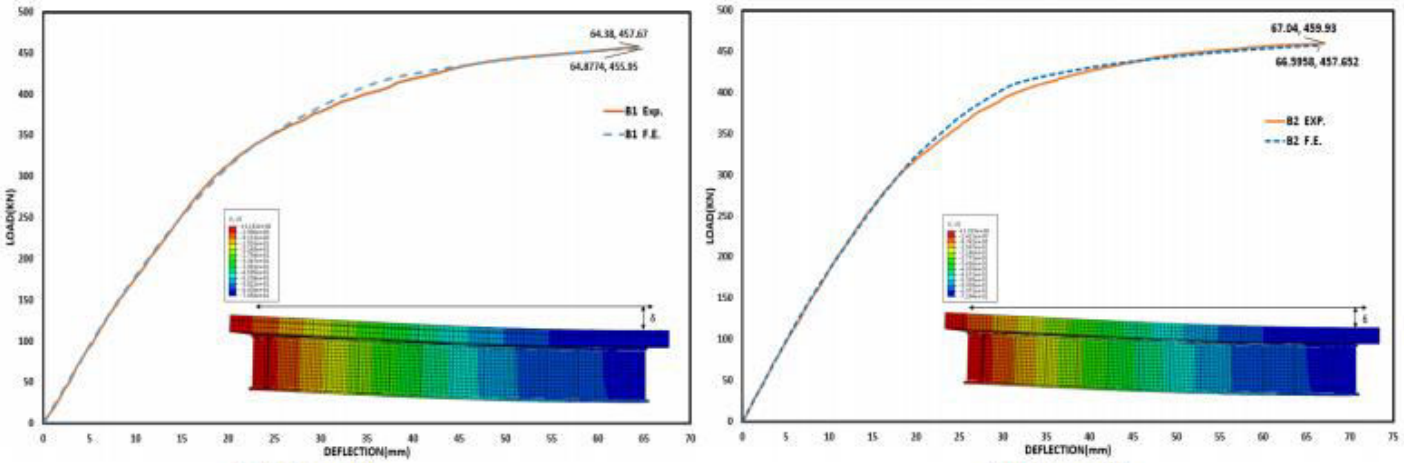

(a) Beam B1 (b) Beam B2

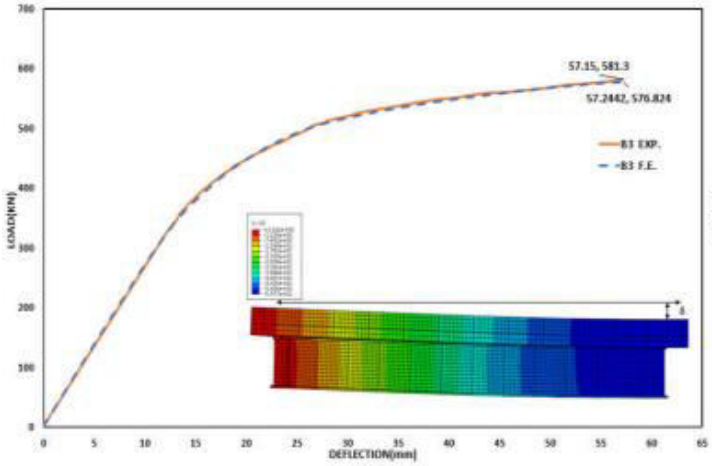

(c) Beam B3

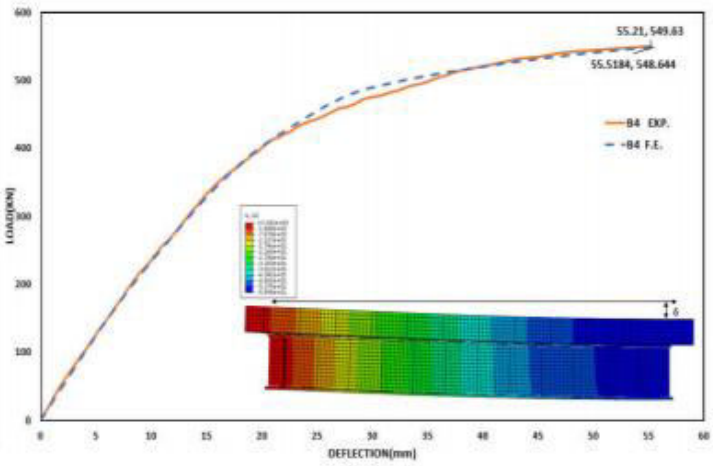

(e) Beam B4

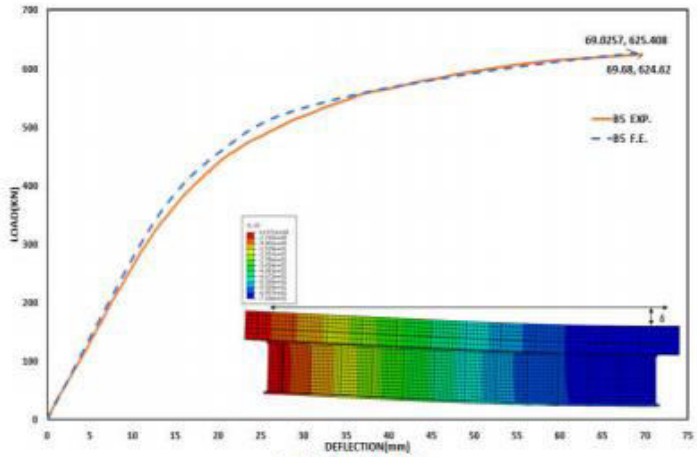

(d) Beam B5

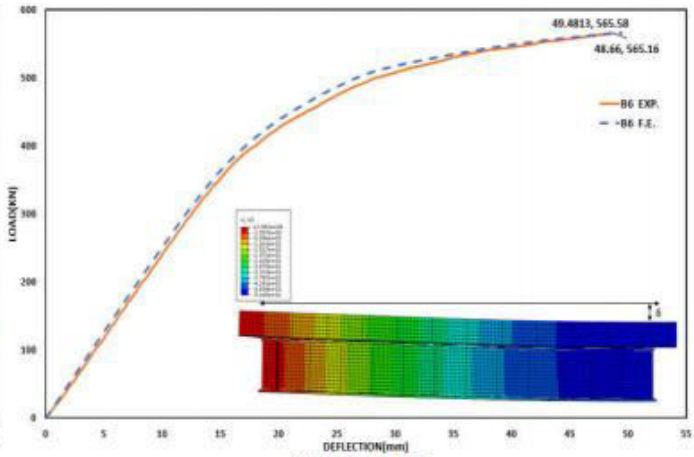

(f) Beam B6

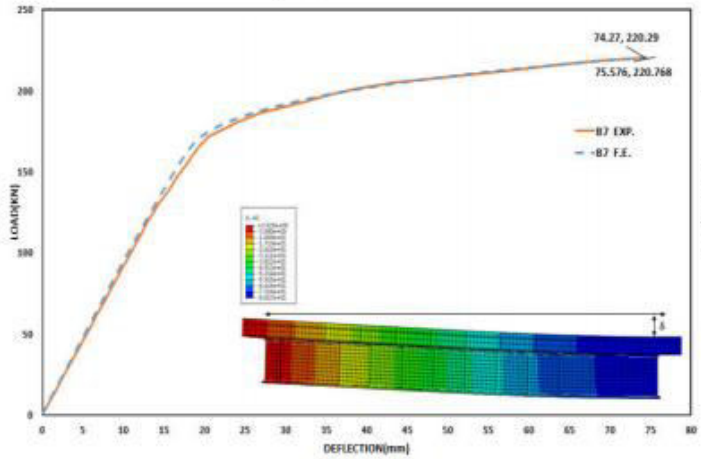

(g) Beam B7

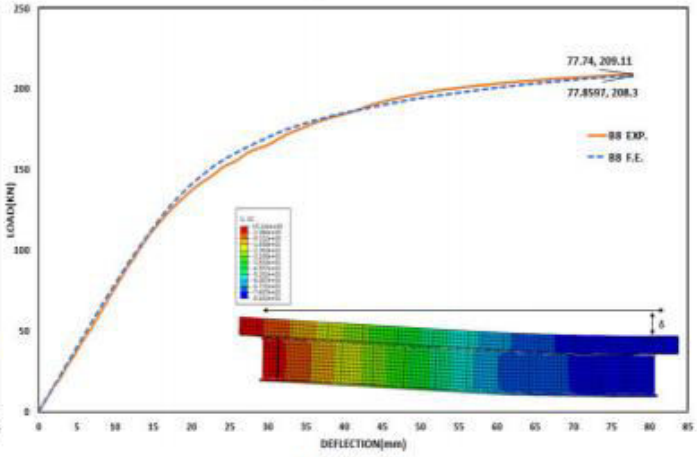

(h) Beam B8

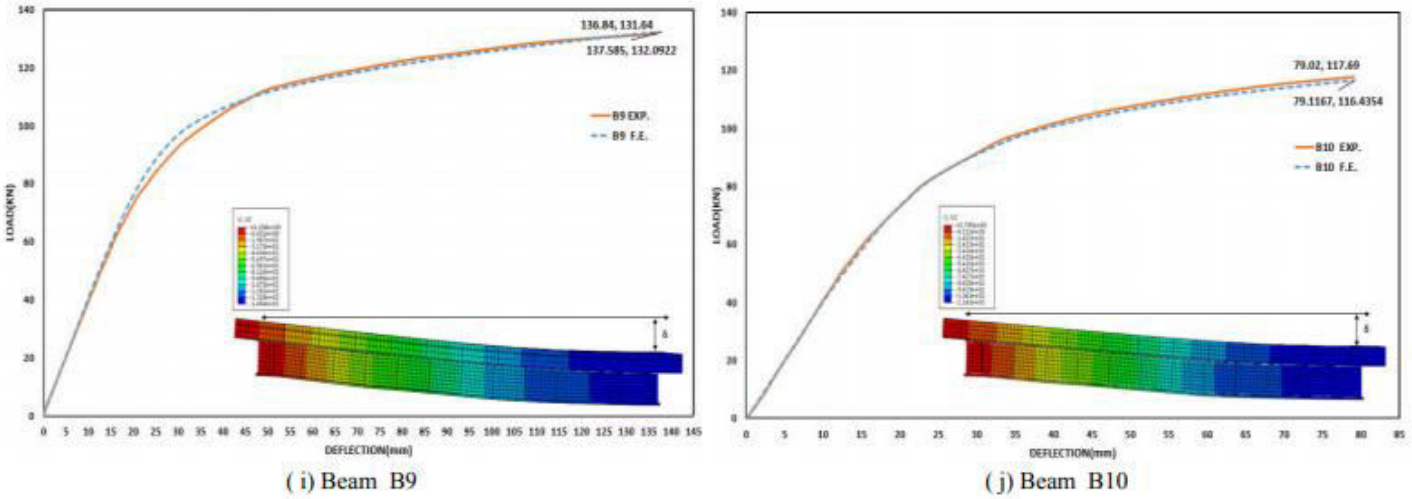

(i) Beam B9 (j) Beam B10

Fig. 4. FEM versus experimental results

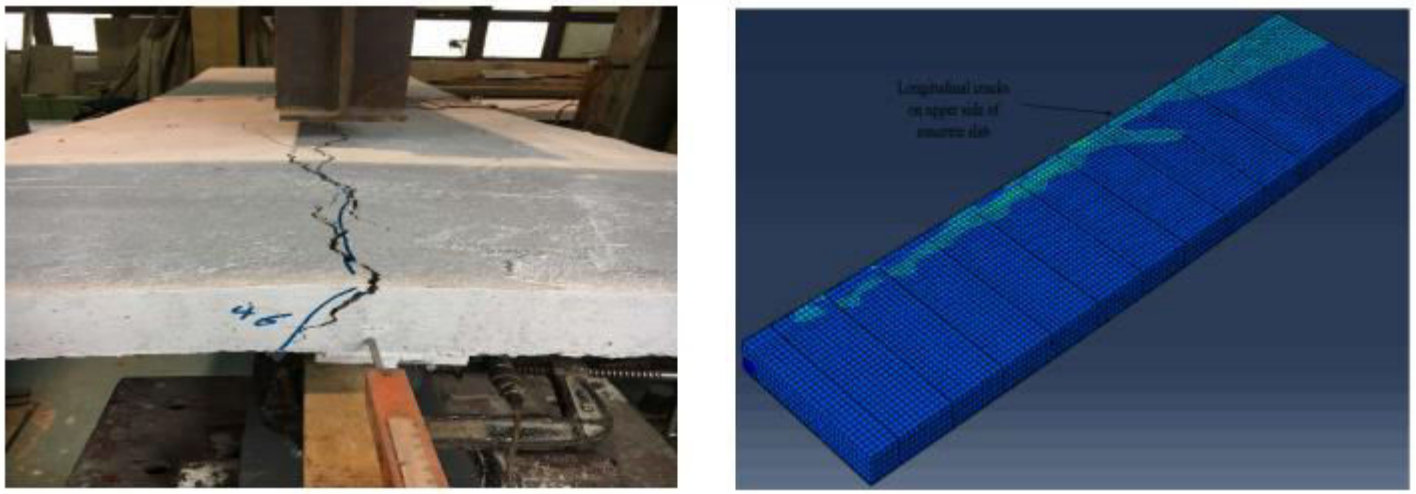

(a) Longitudinal cracks

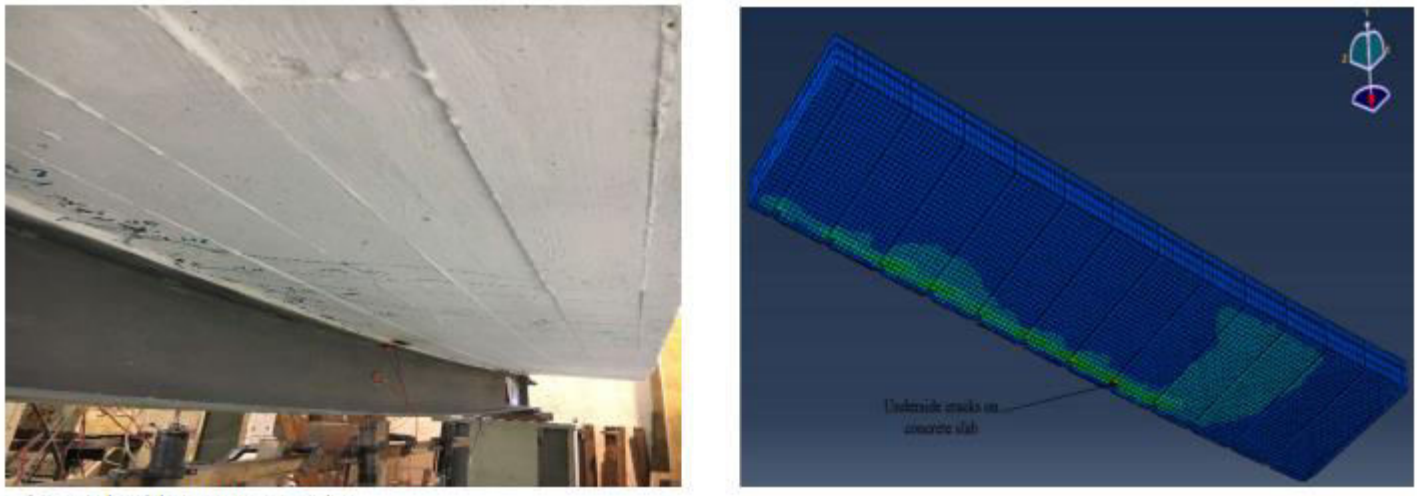

(b) Underside concrete cracks

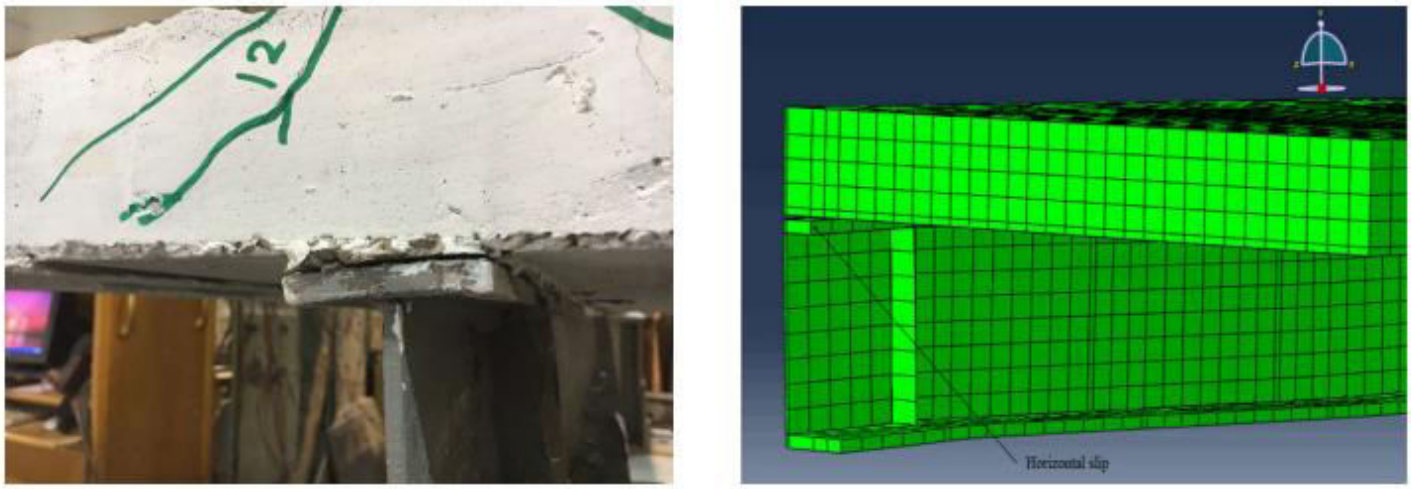

(c) Horizontal slip

Fig. 5. FEM versus experimental failure modes.

Calculation of the effective width of the concrete slab

The effective concrete slab width is calculated based on the numerical model for the ten specimens. The effective concrete slab width is calculated at the elastic stage. The results of calculating the effective concrete slab width from the numerical model will be compared with the experimental results and with the calculation of the effective width in the universal codes (i.e., AISC 360-15, CSA S16-14 and the Eurocode 4; CEN 2004).

The effective concrete slab width is calculated based on the total compressive force in the slab. The total compressive force in the concrete slab (C_{slab}) is calculated using Eq. (1).

$$C_{slab} = \sum_{i=1}^{n} \sigma_i . A_i \qquad (1)$$

where "n" is the number of slab elements, "i" is the element number, "σ" is the longitudinal stress at each element, and "Ai" is the cross-sectional area of the element "i", as shown in Fig. 6.

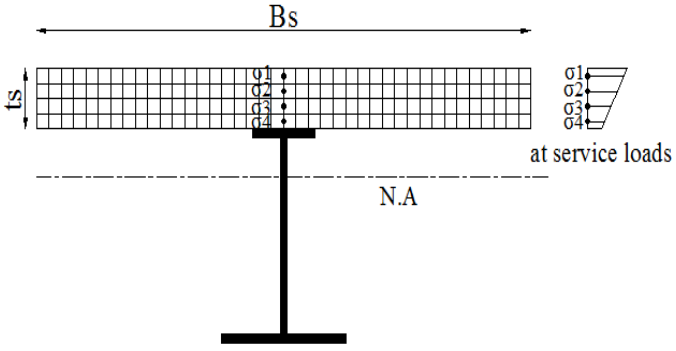

Fig.6. Stress distribution along slab thickness.

The effective concrete slab width can be computed using Eq. (2).

$$B_e = \frac{C_{slab}}{average\ stress\ x\ slab\ thickness} = \frac{C_{slab}}{\frac{\sum \sigma_i}{n} x\ t} \qquad (2)$$

where Be is the total effective slab width for beam and "t" is the total slab thickness, as shown in Fig. 6.

The effective concrete slab width for each SCC beam is determined according to Eq. (2) at the elastic stage, as shown in Table 4. According to results, the effective slab width for all beams from the numerical model exhibited the same trend as the experimental results and with the calculation of the effective width in the universal codes (i.e., AISC 360-15, CSA S16-14 and the Eurocode 4; CEN 2004), as shown in Table 4. Also, the effective concrete slab width for each SCC beam is calculated according to the equation developed by Lasheen et al[23], as shown in Table 4.

The shape of the shear connector has a negligible effect on the value of the effective slab width either at the elastic or plastic stage.From the FEM results, the difference in the effective slab width between beam B1with channel shear connector and beam B2 with angle shear connector is in the range of 4.5%, as shown in Table 4. Also, the difference in the effective slab width between beam B7with channel shear connector and beam B8 with angle shear connector is in the range of 5.5%, as shown in Table 4. For beam B9 with channel shear connector, the difference in the effective slab width is in the range of 7% than beam B10 with angle shear connector, as shown in Table 4. The effect of the slenderness ratio of the steel beam on the effective slab width becomes evident at higher slab width-to-span ratios. Based on its slenderness ratio, the steel beam can use greater effective concrete slab width, where the effective slab width for the SCC beam increases as the slenderness ratio of the steel section decreases, as shown in Table 4. For beam B1with the smallest slenderness ratio (42.2), the beam has used the total slab width in numerical model compare with the code value for the beam with channel shear connector. Also, for beam B2 with the smallest slenderness ratio (42.2), the beam has used 95.6% of the total slab width for the beam with angle shear connector. For beam B9 with the biggest slenderness ratio (70.9), the beam has used 81.3% of the total slab width for the beam with a channel shear connector. For beam B10 with the biggest slenderness ratio (70.9), the beam has used 87.1% of the total slab width for the beam with angle shear connector.

According to the FEM results, the upper steel reinforcement mesh's effect on the effective width of the concrete slab for

beams provided with the channel or the angle shear connectors is slight, as shown in Table 4. For beam B5 with the upper steel reinforcement mesh, the effective width of the concrete slab is higher by 4% than beam B3 without the upper steel reinforcement mesh for the beam with channel shear connector. Also, for beam B6 with the upper steel reinforcement mesh, the effective width of the concrete slab is higher by 0.5% than beam B4 without the upper steel reinforcement mesh for the beam with angle shear connector. The numerical model results showed almost the same trend as the experimental results. The thickness of the concrete slab has a slight effect on the effective concrete slab width. The difference in the effective slab width between beam B1with a slab thickness of 80mm and beam B3 with a slab thickness of 140mm is in the range of 10% for the beam with channel shear connector, as shown in Table 4. Also, the difference in the effective slab width between beam B2 with a slab thickness of 80mm and beam B4 with a slab thickness of 120mm is in the range of 5% for the beam with angle shear connector, as shown in Table 4. The effective slab width from the numerical model has compared with calculating the effective width in the universal codes. For the ANSI/AISC 360-15, the results show that the average difference between the FEM and the results from the ANSI/AISC 360-15 for the effective slab width is in the range of 15%, as shown in Table 4. It should be noted that the 31% and 2% is the maximum and minimum recorded difference in the effective width value between the numerical model and the ANSI/AISC 360-15 in this study, as shown in Fig.7. For the CSA S16-14, the results show that the average difference between the FEM and the results from the CSA S16-14 for the effective slab width is in the range of 2%, as shown in Table 4. The maximum and minimum difference of the effective slabwidth is 16 % and 1% between thenumericalmodel and the CSA S16-14, as shown in Fig.7.

Table 4. Effective slab width at the elastic stageaccording to FEM,Codes limits, ANSI/AISC 360-15, CAN/CSA S16-14 and Eurocode 4; CEN 2004 and Lasheen Equation.

Beam ID	B1	B2	B3	B4	B5	B6	B7	B8	B9	B10
$B_{e\ F.E.}$ (mm)	1200	1147.6	1070.5	1090.8	1109.5	1096.4	1155.7	1095.2	976	1044.7
$B_{ecalc.}$(mm)	1200	1200	1200	1200	1200	1200	1200	1200	1200	1200
% $_{F.E.\ /\ Calc.}$	100	95.6	89.2	90.9	92.5	91.4	96.3	91.3	81.3	87.1
B_{eAISC} (mm)	995.2	1005.6	1048.3	1014.1	1092.6	1046.6	880.0	887.1	824.4	828
% $_{F.E.\ /\ AISC}$	120.6	114.1	102.1	107.5	101.5	104.8	131.3	123.5	118.4	126.1
$B_{eCSA\ (}$mm)	1062.4	1075.7	1198.4	1143.7	1200	1185.1	993	1003.4	965.8	971.4
% $_{F.E.\ /\ CSA}$	112.95	106.7	89.3	95.4	92.5	92.52	116.4	109.1	101.1	107.5
$B_{eEurocode}$ (mm)	1030.5	1041.7	1084.7	1056.5	1145.7	1104.5	952.6	962	937.3	942.6
% $_{F.E.\ /\ Eurocode}$	116.4	110.2	98.7	103.2	96.8	99.3	121.3	113.8	104.1	110.8
$B_{elasheen\ Eq.}$ (mm)	1126.2	1126.2	1126.2	1126.2	1126.2	1126.2	1048.5	1048.5	982.8	982.8
% $_{F.E.\ /lasheen\ Eq}$	106.5	101.9	95.1	96.85	98.52	97.4	110.2	104.4	99.3	106.3

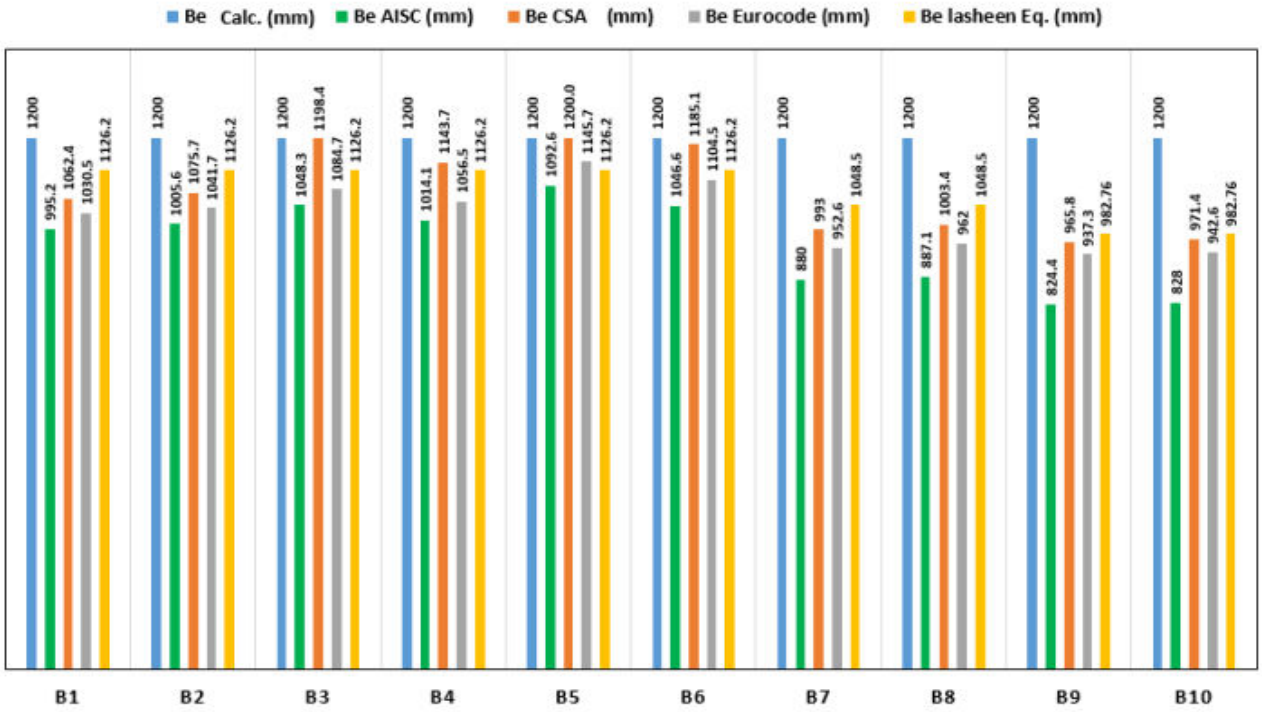

Fig.7. Comparison between the effective width of the concrete slab at the elastic stageaccording to FEM, Codes limits, ANSI/AISC 360-15, CAN/CSA S16-14 and Eurocode 4; CEN 2004 and Lasheen Equation.

For Eurocode 4; CEN 2004, the results show that the average difference between the FEM and the results from the Eurocode 4; CEN 2004 for the effective slab width is in the range of 7%, as shown in Table 4. The maximum and minimum difference of the effective slab width is 21 % and 1% between the numerical model and the Eurocode 4; CEN 2004, as shown in Fig.7. The effective slab width from the numerical model has also compared with the effective width calculation according to the equation developed by Lasheen et al. The results show that the numerical model agrees with Lasheen equation. The average difference between the FEM and Lasheen equation results for the effective slab width is in the range of 2 %, as shown in Table 4. It can be noted that the 10% and 1% is the maximum and minimum recorded difference in the effective slab width value between the numerical model and Lasheen equation, as shown in Fig.7. This confirms the suitability of Lasheen equation for calculating the effective slab width for mono symmetric steel sections provided with either channel or angle shear connector.

Parametric study

A parametric study is conducted on ten beams to evaluate the contribution of using the upper reinforced steel mesh on the load capacity of a mono-symmetric steel section. Also, to study the effect of top mesh on the effective slab width of a mono-symmetric steel section and compares the results with the codes limit. As shown in Table 5, the mono-symmetrical steel beams with a total length of 5000 mm were simply supported with a 4800 mm clear span. The span-to-composite section depth ratio (L/d) is calculated for all beams, as shown in Table 5. Also, the ratio between slab width to span (B_S/L) and the slenderness ratio (L/rs) is equal to 0.25 and 42.15, respectively, for all beams. The connectors' spacing of all beams is 200 mm. According to Table 5 and Fig.8, Five beams have a concrete slab thickness of 120 mm and the other five beams have aconcrete slab thickness of 140 mm. All beams have concrete slab width of 1200 mm. The lower reinforcement of concrete slabs is a mesh of 8 mm diameter and 200 mm spacing in both longitudinal and transverse directions for all beams. The upper reinforcement of concrete slabs is a variable, as shown in Table 5 with 200 mm spacing in both longitudinal and transverse directions. It should be noted that the ratio between the area of upper steel mesh to the area of the concrete slab is varying from 0.18% to 0.91% for beams with channel shear connectors and varying from 0.21% to 1.06% for beams with angle shear connectors. The main testing parameters are the upper steel reinforcement mesh, the different shapes of shear connectors (i.e., channel and angle) and the thickness of the concrete slab, as shown in Fig. 8.

Results

The results of the current parametric study will be discussed in this section for all beams models. This section illustrates the effect of using the upper steel reinforcement mesh on the behaviour of the SCC beams. Also, this section presents the relation between the ratio of the upper steel reinforcement mesh and the behaviour of the SCC beams. Besides, it is presented a relation between the ratio of the upper steel reinforcement mesh and the concrete slab effective width. Moreover, the effect of the upper steel reinforcement mesh on the SCC beams' slip value is investigated with different shapes of shear connectors (i.e., channel or angle). A summary of parametric study results, including the ultimate load, mid-span deflection value at yield and ultimate, slip value at the steel-concrete interface at yield and ultimate and the effective concrete slab width, are presented in Table 6. The results are presented in terms of the load-deflection, load-steel strain, load-concrete strain and load-slip value. The results for all beams are illustrated in Fig.9.

Effect of the upper steel reinforcement mesh on the ultimate load

From the results, it can be noted that the beams' failure load increased with increasing the ratio of the upper steel reinforcement mesh.As shown in Fig. 10,for beam B51 with upper steel reinforcement mesh with a ratio of 0.18% from the area of the concrete slab, the failure load is higher than that of the beam without upper steel reinforcement mesh by 7.9 % for beams with channel shear connector, where the failure load is 622.58 kN for beam B51. For beam B52 with upper steel reinforcement mesh with a ratio of 0.28% from the area of the concrete slab, the failure load is higher than that of the beam without upper steel reinforcement mesh by 8.4 %, where the failure load is 625.4 kN for beam B52. For beam B53 with upper steel reinforcement mesh with a ratio of 0.4% from the area of the concrete slab, the failure load is higher than that of the beam without upper steel reinforcement mesh by 9 %, where the failure load is 628.8 kN for beam B53. For beam B54 with upper steel reinforcement mesh with a ratio of 0.72% from the area of the concrete slab, the failure load is higher than that of the beam without upper steel reinforcement mesh by 10.1 %, where the failure load is 635.1 kN for beam B54. For beam B55 with upper steel reinforcement mesh with a ratio of 0.91% from the area of the concrete slab, the failure load is higher than that of the beam without upper steel reinforcement mesh by 10.4 %, where the failure load is 636.9 kN for beam B55. Also, for beams with anangle shear connector, the failure load increased with increasing the ratio of the upper steel reinforcement mesh. For beam B61 with upper steel reinforcement mesh with a ratio of 0.21% from the area of the concrete slab, the failure load is higher than that of the beam without upper steel reinforcement mesh by 2.65%, where the failure load is 563.2kN for beam B61.For beam B62 with upper steel reinforcement mesh with a ratio of 0.33% from the area of the concrete slab, the failure load is higher than that of the beam without upper steel reinforcement mesh by 3.1%, where the failure load is 565.6 kN for beam B62. For beam B63 with upper steel reinforcement mesh with a ratio of 0.47% from the area of the concrete slab, the failure load is higher than that of the beam without upper steel reinforcement mesh by 3.6 %, where the failure load is 568.4 kN for beam B63.For beam B64 with upper steelreinforcement mesh with a ratio of 0.84% from the area of the concrete slab, the failure load is higher than that of the beam without upper steel reinforcement mesh by 4.3 %, where the failure load is 572.2 kN for beam B64.For beam B65 with upper steel reinforcement mesh with a ratio of 1.06% from the area of the concrete slab, the failure load is higher than that of the beam without upper steel reinforcement mesh by 4.74 %, where the failure load is 574.6 kN for beam B65.

Effect of the upper steel reinforcement mesh on mid-span deflection value.

The presence of upper steel reinforcement mesh reduces deflection due to a reduction of cracks along the total span. As shown in Fig. 11, for beam B51 with upper steel reinforcement

mesh with a ratio of 0.18% from the area of the concrete slab, the vertical deflection decreased by 18.5 % at the ultimate load of the beam without upper steel reinforcement mesh for beams with channel shear connector. The recorded vertical deflection values for beam B51 with upper steel reinforcement mesh and the beam without upper steel reinforcement mesh are 46.61 mm and 57.24 mm, respectively.

For beam B52 with upper steel reinforcement mesh with a ratio of 0.28% from the area of the concrete slab, the vertical deflection decreased by 19 % at the ultimate load of the beam without upper steel reinforcement mesh, where the recorded vertical deflection value for beam B52 is 46.36 mm. For beam B53 with upper longitudinal steel with a ratio of 0.4% from the area of the concrete slab, the vertical deflection decreased by 23.5 % at the ultimate load of the beam without upper steel reinforcement mesh, where the recorded vertical deflection value for beam B53 is 43.79 mm. For beam B54 with upper longitudinal steel with a ratio of 0.72% from the area of the concrete slab, the vertical deflection decreased by 27.45 % at the ultimate load of the beam without upper steel reinforcement mesh, where the recorded vertical deflection value for beam B54 is 41.53 mm. For beam B55 with upper longitudinal steel with a ratio of 0.91% from the area of the concrete slab, the vertical deflection decreased by 32.5 % at the ultimate load of the beam without upper steel reinforcement mesh, where the recorded vertical deflection value for beam B55 is 38.63 mm. Also, for beam B61 with upper longitudinal steel with a ratio of 0.21% from the area of the concrete slab, the vertical deflection decreased by 22.4 % at the ultimate load of the beam without upper steel reinforcement mesh for beams with angle shear connector.

The recorded vertical deflection values for beam B61 with upper longitudinal steel and beam without upper longitudinal steel are 43.1 mm and 55.52 mm, respectively. For beam B62 with upper longitudinal steel with a ratio of 0.33% from the area of the concrete slab, the vertical deflection decreased by 24.2 % at the ultimate load of the beam without upper steel reinforcement mesh, where the recorded vertical deflection value for beam B62 is 42.1mm. For beam B63 with upper longitudinal steel with a ratio of 0.47% from the area of the concrete slab, the vertical deflection decreased by 29.7 % at the ultimate load of the beam without upper steel reinforcement mesh, where the recorded vertical deflection value for beam B63 is 39.02 mm. For beam B64 with upper longitudinal steel with a ratio of 0.84% from the area of the concrete slab, the vertical deflection decreased by 36.1 % at the ultimate load of the beam without upper steel reinforcement mesh, where the recorded vertical deflection value for beam B64 is 35.45 mm. For beam B65 with upper longitudinal steel with a ratio of 1.06% from the area of the concrete slab, the vertical deflection decreased by 43.75 % at the ultimate load of the beam without upper steel reinforcement mesh,where the recorded vertical deflection value for beam B65 is 31.23 mm.

Effect of the upper steel reinforcement mesh on slip value.

The existence of upper steel reinforcement mesh reduces the slip value between the concrete slab and the steel section due to a reduction of cracks in the concrete slab. As shown in Fig. 12, for beam B51, with upper steel reinforcement mesh with a ratio of 0.18% from the area of the concrete slab, the slip value decreased by 51.2 % at the ultimate load of the beam without upper steel reinforcement mesh for beams with channel shear connector. The recorded slip values for beam B51 with upper steel reinforcement mesh and beam without upper steel reinforcement mesh are 0.4 mm and 0.81 mm, respectively. For beam B52 with upper steel reinforcement mesh with a ratio of 0.28% from the area of the concrete slab, the slip value decreased by 56.2 % at the ultimate load of the beam without upper steel reinforcement mesh. The recorded slip value for beam B52 is 0.36 mm. For beam B53 with upper steel reinforcement mesh with a ratio of 0.4% from the area of the concrete slab, the slip value decreased by 57.5 % at the ultimate load of the beam without upper steel reinforcement mesh. The recorded slip value for beam B53 is 0.345 mm. For beam B54 with upper steel reinforcement mesh with a ratio of 0.72% from the area of the concrete slab, the slip value decreased by 59.4 % at the ultimate load of the beam without upper steel reinforcement mesh. The recorded slip value for beam B54 is 0.33 mm. For beam B55 with upper steel reinforcement mesh with a ratio of 0.91% from the area of the concrete slab, the slip value decreased by 60 % at the ultimate load of the beam without upper steel reinforcement mesh. The recorded slip value for beam B55 is 0.32 mm. Also, for beam B61 with upper steel reinforcement mesh with a ratio of 0.21% from the area of the concrete slab, the slip value decreased by 40.2% at the ultimate load of the beam without upper steel reinforcement mesh for beams with angle shear connector. The recorded slip values for beam B61 with upper steel reinforcement mesh and beam without upper steel reinforcement mesh are 0.53 mm and 0.88 mm, respectively. For beam B62 with upper steel reinforcement mesh with a ratio of 0.33% from the area of the concrete slab, the slip value decreased by 45.9% at the ultimate load of the beam without upper steel reinforcement mesh, where the recorded slip value for beam B62 is 0.48 mm. For beam B63 with upper steel reinforcement mesh with a ratio of 0.47% from the area of the concrete slab, the slip value decreased by 53.2 % at the ultimate load of the beam without upper steel reinforcement mesh, where the recorded slip value for beam B63 is 0.41 mm.

For beam B64 with upper steel reinforcement mesh with a ratio of 0.84% from the area of the concrete slab, the slip value decreased by 56.1 % at the ultimate load of the beam without upper steel reinforcement mesh, where the recorded slip value for beam B64 is 0.39 mm. For beam B65 with upper steel reinforcement mesh with a ratio of 1.06% from the area of the concrete slab, the slip valuedecreased by 56.8 % at the ultimate load of the beam without upper steel reinforcement mesh, where the recorded slip value for beam B65 is 0.38 mm.

Effect of the upper steel reinforcement mesh on the effective concrete slab width.

The effect of having different upper steel reinforcement mesh ratios on the value of the effective slab width is studied in this section. The results showed that the effect of the upper steel reinforcement mesh on the effective width of the concrete slab is slight for beams provided with the channel or the angle shear connector. As shown in Fig. 13, for beam B51, with upper steel reinforcement mesh with a ratio of 0.18% from the area of the concrete slab, the effective slab width value increased by 2.5 %

at the service load of the beam without upper steel reinforcement mesh for beams with channel shear connector. The effective slab width values for beam B51 with upper steel reinforcement mesh and beam without upper steel reinforcement mesh are 1097.4 mm and 1070.5 mm, respectively.

For beam B52 with upper steel reinforcement mesh with a ratio of 0.28% from the area of the concrete slab, the effective slab width value increased by 3.64 % at the service load of the beam without upper steel reinforcement mesh, where the effective slab width value for beam B52 is 1109.5 mm. For beam B53 with upper steel reinforcement mesh with a ratio of 0.4% from the area of the concrete slab, the effective slab width value increased by 5.2 % at the service load of the beam without upper steel reinforcement mesh, where the effective slab width value for beam B53 is 1126 mm. For beam B54 with upper steel reinforcement mesh with a ratio of 0.72% from the area of the concrete slab, the effective slab width value increased by 7.7 % at the service load of the beam without upper steel reinforcement mesh, where the effective slab width value for beam B54 is 1152.8 mm.

For beam B55 with upper steel reinforcement mesh with a ratio of 0.91% from the area of the concrete slab, the effective slab width value increased by 9.1% at the service load of the beam without upper steel reinforcement mesh, where the effective slab width value for beam B55 is 1167.6 mm. For beams with angle shear connectors, the effect of using upper steel reinforcement mesh is slight. For beam B61, with upper steel reinforcement mesh with a ratio of 0.21% from the area of the concrete slab, the effective slab width value is slightly higher than the beam without upper steel reinforcement mesh at service load.

The effective slab width values for beam B61 with upper steel reinforcement mesh and beam without upper steel reinforcement mesh are 1092.2 mm and 1090.8 mm, respectively. For beam B62 with upper steel reinforcement mesh with a ratio of 0.33% from the area of the concrete slab, the effective slab width value increased by 0.5 % at the service load of the beam without upper steel reinforcement mesh, where the effective slab width value for beam B62 is 1096.4 mm. For beam B63 with upper steel reinforcement mesh with a ratio of 0.47% from the area of the concrete slab, the effective slab width value increased by 0.75 % at the service load of the beam without upper steel reinforcement mesh, where the effective slab width value for beam B63 is 1098.9 mm. For beam B64 with upper steel reinforcement mesh with a ratio of 0.84% from the area of the concrete slab, the effective slab width value increased by 1.5 % at the service load of the beam without upper steel reinforcement mesh, where the effective slab width value for beam B64 is 1107.3 mm.

For beam B65 with upper steel reinforcement mesh with a ratio of 1.06% from the area of the concrete slab, the effective slab width value increased by 1.72 % at the service load of the beam without upper steel reinforcement mesh, where the effective slab width value for beam B65 is 1109.6 mm.

Conclusions

This study has shown that the results of the finite element model show perfect agreement with the experimental results. The following conclusions are drawn:

1.The results of the FEM are precisely consistent with the experimental results. The FEM results showed that the average ratio between the FE and experimental results for ultimate loads is 99.75%and with a difference of 0.41 % in deflection value.

2.The FEM results showed that the shape of the shear connector has a negligible effect on the value of the effective slab width, where the average difference in the effective slab width between beams with channel shear connector and beams with angle shear connector is in the range of 5.6%.

3.The results of the FEM Proved that the effective slab width for beams decreases as the slenderness ratio of the steel section increases. The increase of the slenderness ratio of the steel section by 68% decreases the effective slab width by 19% for the beams with channel shear connector and by 9% for the beams with angle shear connector. Also, the increase of the slenderness ratio of the steel section by 31% leads to decreases in the effective slab width by 4% for the beams with channel shear connector and by 5% for the beams with angle shear connector.

4. The results of the FEM showed that the increase in the ratio of the upper steel reinforcement mesh affectsthe value of the ultimate load, mid-span deflection value and the slip value at the steel-concrete interface.

5. The effective width of the concrete slab for beams provided with the channel or the angle shear connectors increaseswith the increase in the ratio of the upper steel reinforcement mesh.

6. The presence of upper steel reinforcement mesh reduces the slip value between the concrete slab and the steel. For beams with channel shear connectors, The presence of upper steel reinforcement mesh with a ratio of 0.91% from the area of the concrete slab leads to decreased the slip value by 60 % at the ultimate load of the beam without upper steel reinforcement mesh.

7. The presence of upper steel reinforcement mesh with a ratio of 0.91% from the area of the concrete slab leads to decreased vertical deflection by 32.5 % at the ultimate load of the beam without upper steel reinforcement for beams with channel shear connectors.

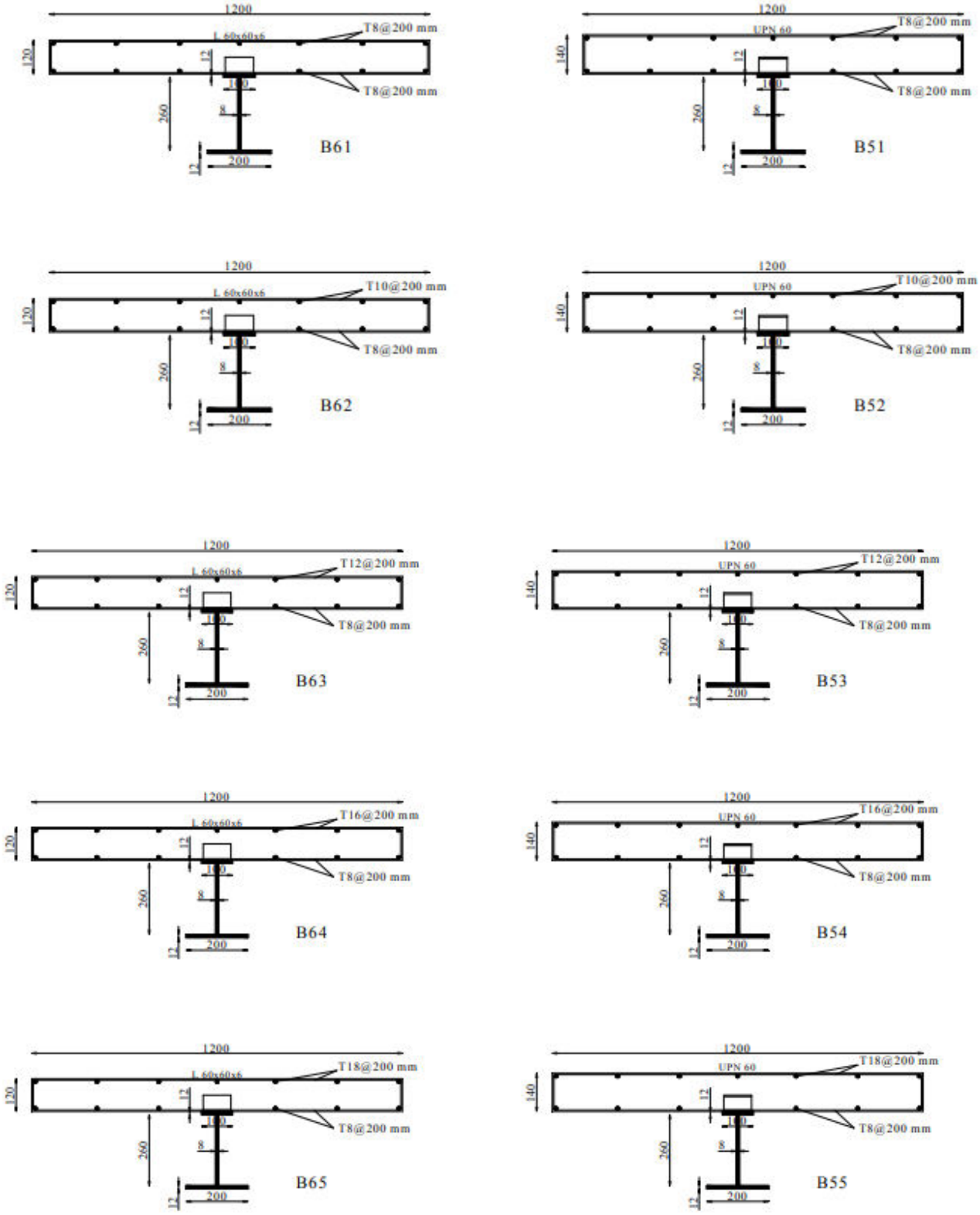

Fig. 8. Variables of the parametric study.

Table 5. Details of beams in the parametric study.

Beam ID	Total Length (mm)	Span, L (mm)	Slab width, Bs(mm)	slab thickness, ts(mm)	Connector shape	h w (mm)	t w (mm)	t f (mm)	b L (mm)	b u (mm)	L/rs	L/d	Upper transverse steel
B51				140	UPN 60							11.32	With
B61				120	Angle 60							11.88	5Ø8/m
B52				140	UPN 60							11.32	With
B62				120	Angle 60							11.88	5Ø10/m
B53	5000	4800	1200	140	UPN 60	260	8	12	200	100	42.2	11.32	With
B63				120	Angle 60							11.88	5Ø12/m
B54				140	UPN 60							11.32	With
B64				120	Angle 60							11.88	5Ø16/m
B55				140	UPN 60							11.32	With
B65				120	Angle 60							11.88	5Ø18/m

Table 6. Summary of test results of beams in the parametric study.

Beam ID	Concrete Slab Failure Mode-load					Effective width (Be) (mm.)
	Failure Load (kN)	Deflection at yield (mm.)	Deflection at ultimate (mm.)	Slip Value at yield (mm.)	Slip Value at Ultimate (mm.)	
B51	622.58	13.88	72.69	0.166	0.81	1097.4
B52	625.41	13.76	69.03	0.165	0.79	1109.5
B53	628.82	13.66	66.67	0.165	0.8	1126
B54	635.1	13.33	63.46	0.165	0.88	1152.8
B55	636.92	13.25	61.68	0.164	0.88	1167.6
B61	563.2	15.87	51.53	0.185	0.84	1092.2
B62	565.58	15.77	49.48	0.185	0.84	1096.4
B63	568.42	15.59	48.4	0.185	0.84	1098.9
B64	572.16	15.29	44.87	0.183	0.83	1107.3
B65	574.64	15.09	44.49	0.181	0.94	1109.6

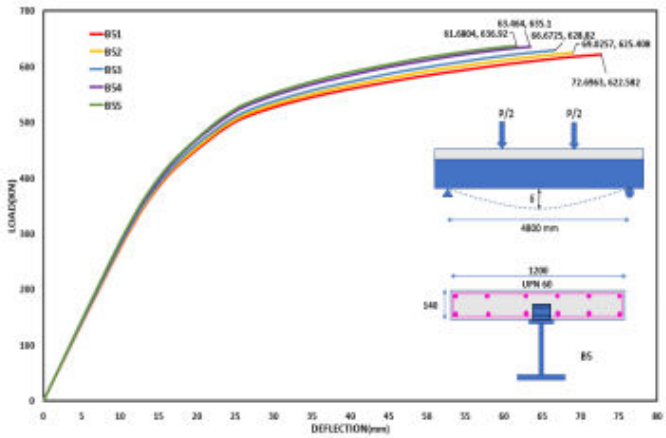

(a) Load versus mid-span deflection for beams B51 to B55.

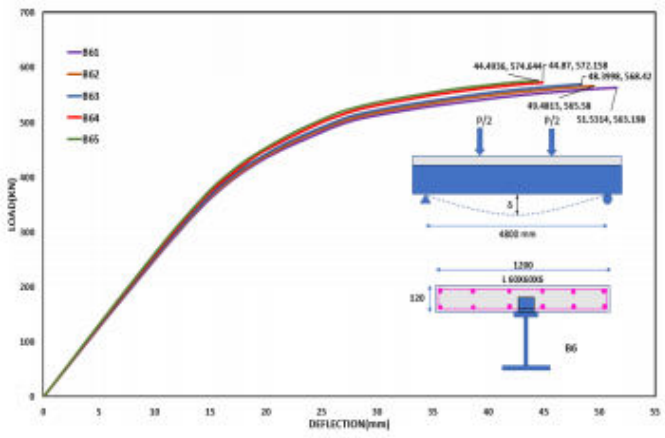

(b) Load versus mid-span deflection for beams B61 to B65.

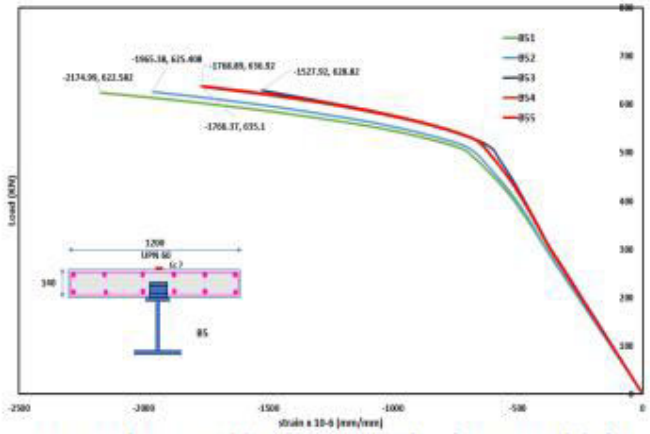

(c) Load versus mid-span upper strain of concrete slab for beams B51 to B55.

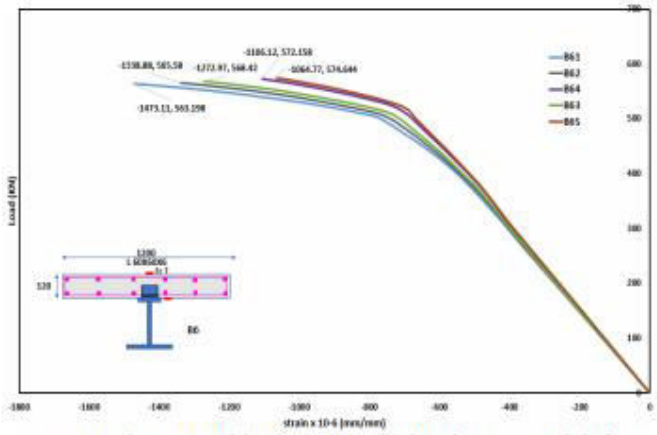

(d) Load versus mid-span upper strain of concrete slab for beams B61 to B65.

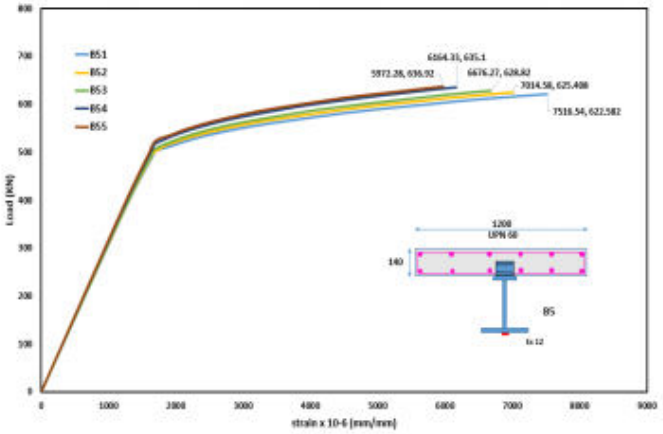

(e) Load versus mid-span strain at steel lower flange for beams B51 to B55.

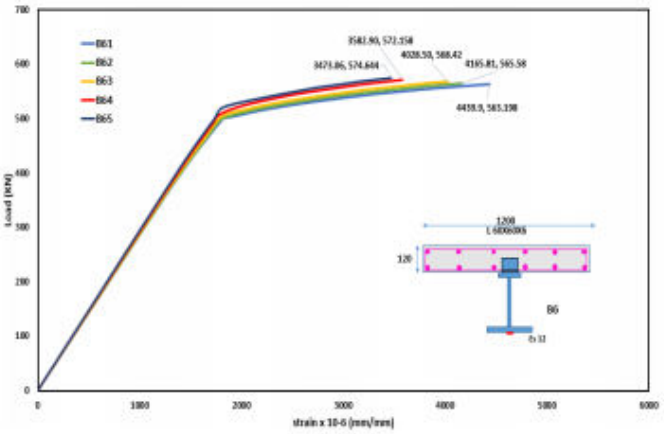

(f) Load versus mid-span strain at steel lower flange for beams B61 to B65.

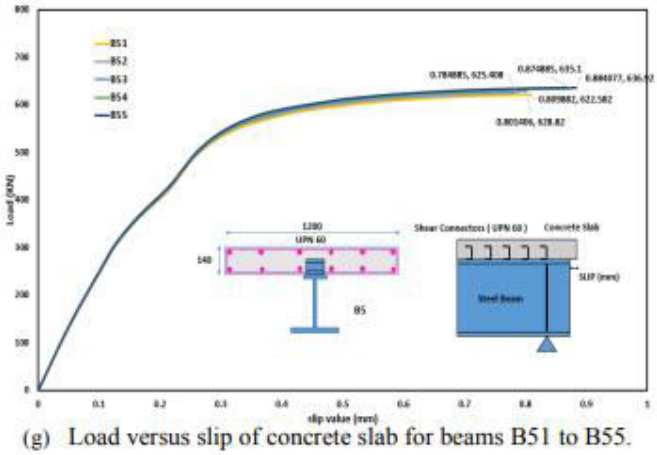

(g) Load versus slip of concrete slab for beams B51 to B55.

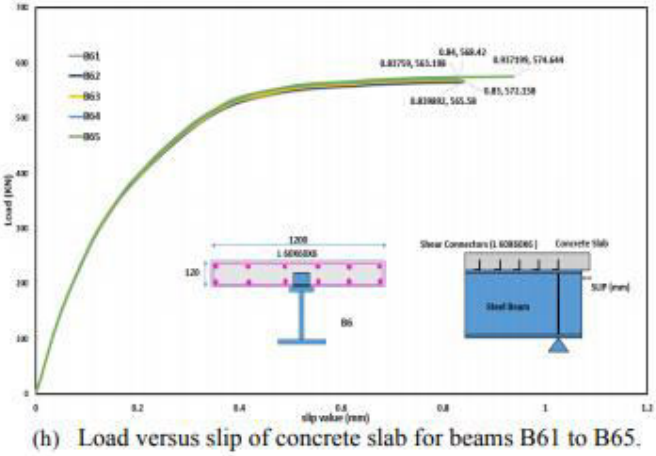

(h) Load versus slip of concrete slab for beams B61 to B65.

Fig. 9. Numerical results for all beams.

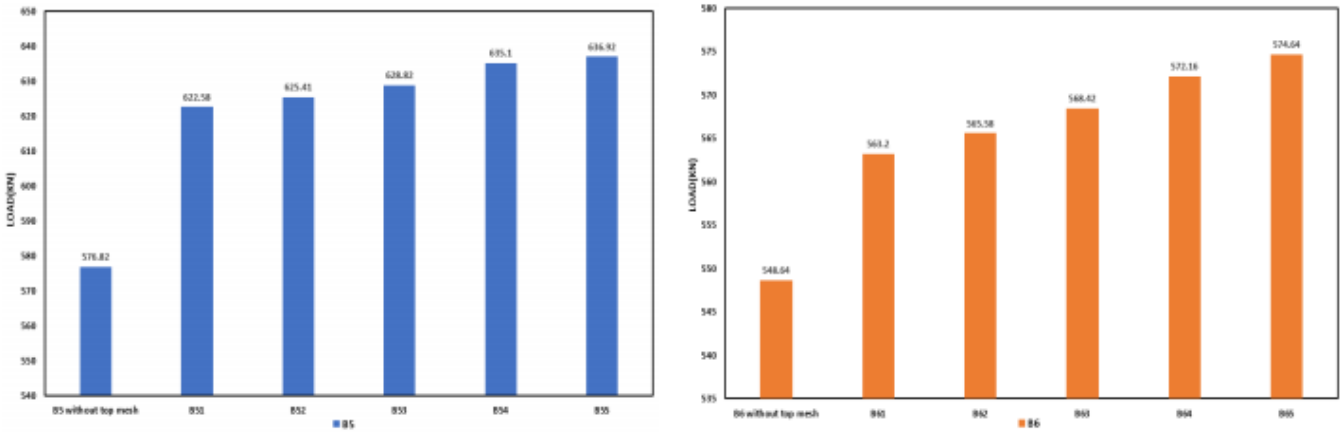

(a) Comparison of the failure load for the specimens (B5) with and without top mesh.

(b) Comparison of the failure load for the specimens (B6) with and without top mesh.

Fig. 10. Effect of the upper steel reinforcement mesh on ultimate load capacity

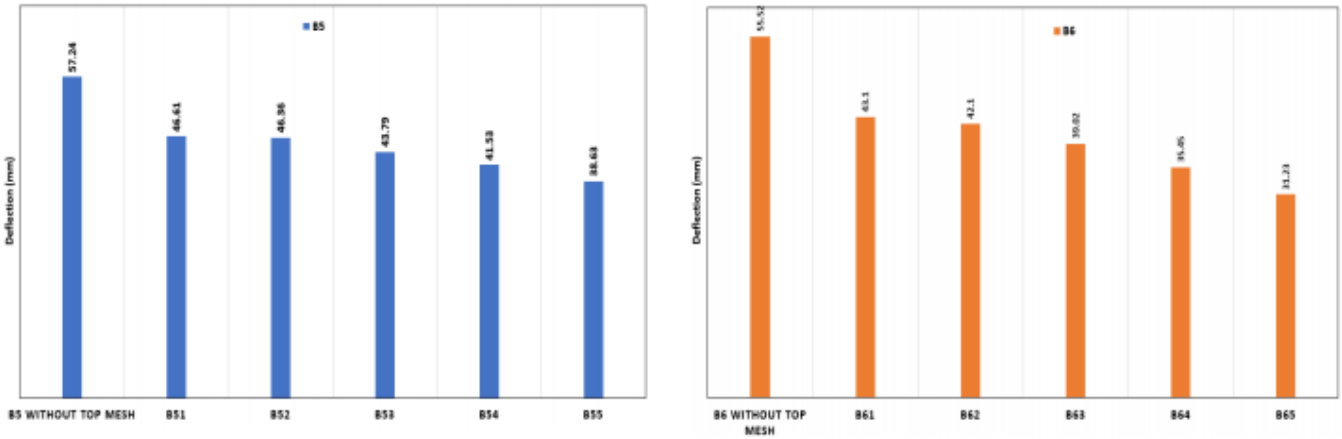

(a) Comparison of the deflection for the specimens (B5) with and without top mesh.

(b) Comparison of the deflection for the specimens (B6) with and without top mesh.

Fig.11 Effect of the upper steel reinforcement mesh on deflection value.

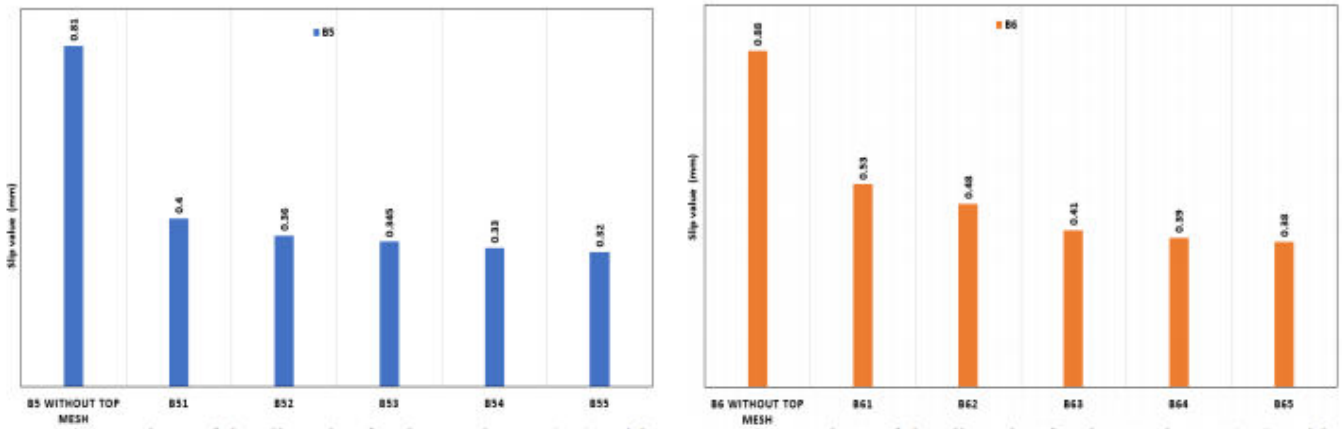

(a) Comparison of the slip value for the specimens (B5) with and without mesh.

(b) Comparison of the slip value for the specimens (B6) with and without top mesh.

Fig.12 Effect of the upper steel reinforcement mesh on slip value

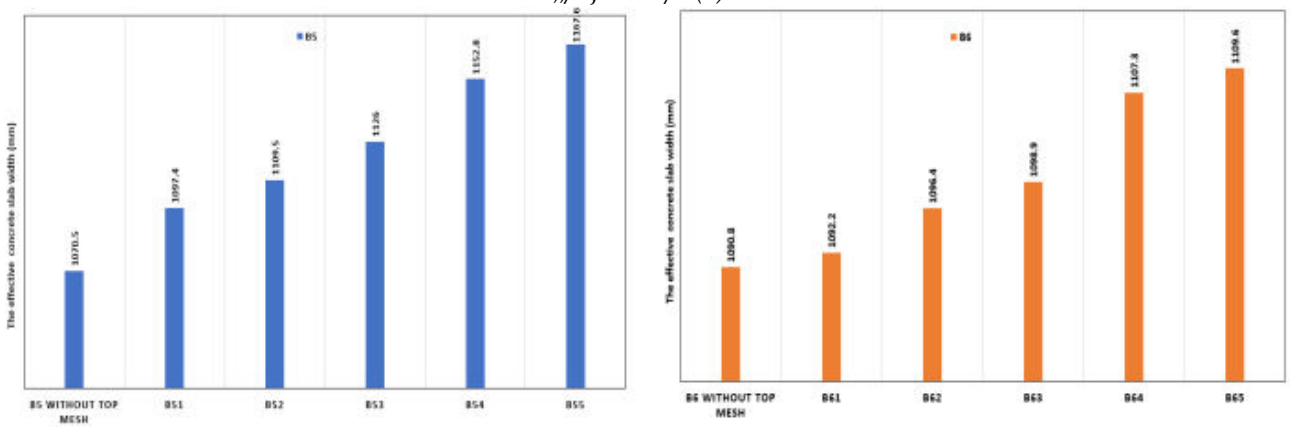

(a) Comparison of the effective concrete slab width for the specimens (B5 with and without top mesh.

(b) Comparison of the effective concrete slab width for the specimens (B6) with and without top mesh.

Fig.13 Effect of the upper steel reinforcement mesh on the effective concrete slab width.

References

[1] J. He, Y. Liu, A. Chen, and T. Yoda, Experimental study on
inelastic mechanical behaviour of composite girders under hogging moment, Journal of Constructional Steel Research, 66(1), 2010, pp. 37-52.

[2] A.S. Larbi, A. Ferrier, and P. Hamelin, Concrete to steel lap
joint failure criteria under combined shear and peeling stress, Journal of Constructional Steel Research, 65(2), 2009, pp. 386-394.

[3] J. Nie, C.S. Cai, Steel-Concrete composite beams considering shear slip effects, J.Struct.Eng., ASCE 129 (4) (2003) 495–506.

[4]Raguvaran Balasubramanian, Baskar Rajaram, Int, J. Steel Struct. 16, 807–811(2016).

[5] Kamar, Ahmed, MahmoudLasheen,Amr Shaat,Amr zaher, and Ayman Khalil. "Behaviour of Mono-symmetric Steel-concrete Composite Section provided withAngle and Channel Shear connectors" International Journal of Research in Engineering &Management 4(1), 2020, pp. 36-51.

[6] N. Gattesco, "Analytical modelling of nonlinear behaviour of composite beams with deformable connection" Journal of Constructional Steel Research, 1999, vol. 52, pp. 195–218

[7] H.Y. Loh, and M.A. Bradford, "The effect of partial connection in the hogging moment region of composite beams Part II-Analytical study", Journal of constructional Steel Research, 2004, vol. 60, pp. 921-962

[8] R. Seracino, C.T. Lee, Z. Tan, "Partial interaction shear flow forces in continuous composite steel-concrete beams", Journal of structural engineering, ASCE, 2006, vol. 132, No. 2, pp. 227-236.

[9] G. Ranzi and A. Zona, "A steel–concrete composite beam model with partial interaction including the sheardeformability of the steel component", EngineeringStructures, 2007, vol. 29, pp. 3026–3041

[10] Maleki, Shervin, and Mehrdad Mahoutian. "Experimental and analytical study on channel shear connectors in fiber-reinforced concrete." Journal of Constructional Steel Research 65.8-9 (2009): 1787-1793.

[11] Prakash, Amar, et al. "Three-dimensional FE model of stud connected steel-concrete composite girders subjected to monotonic loading." International Journal of Mechanics and Applications 1.1 (2011): 1-11.

[12] Tahmasebinia, Faham, Gianluca Ranzi, and Alessandro Zona. "Beam tests of composite steel-concrete members: A three-dimensional finite element model." International Journal of Steel Structures 12.1 (2012): 37-45.

[13] M. Chiewanichakorn, A. Aref, S. Chen, I. Ahn, Effective flange width definition for steel– concrete composite bridge Girder, J. Struct. Eng., ASCE 130 (12) (2004) 2016–2031.

[14] American Institute of Steel Construction, ANSI/AISC-360-15.Specification for Structural Steel Buildings, Chicago, Illinois.

[15] Canadian Standards Association, CAN/CSA-S16-14, Limit states design of steel structures, Mississauga, Ontario.

[16] C. Amadio, C. Fedrigo, M. Fragiacomo, L. Macorini, Experimental evaluation of effective width in steel–concrete composite beams, J. Constr. Steel Res. 60 (2) (2004) 199–220.

[17] Lasheen, Mahmoud, Amr Shaat, and Ayman Khalil. "Behaviour of lightweight concrete slabs acting compositely with steel I-sections." Construction and Building Materials 124 (2016): 967-981.

[18] Eurocode, Design of Composite Steel and Concrete Structures. Part 1. 1: General Rules and Rules for Buildings, 2004.

[19] ABAQUS, Theory Manual Version 6.14, Dassault Systemes, 2014.

[20] K. Baskar, N.E. Shanmugam, Thevendran, Finite element analysis of steel-concretecomposite plate girder J. Struct. Eng. ASCE 128 (9) (2002) 1158–1168.

[21] Q.Q. Liang, B. Uy, M.A. Bradford, H.R. Ronagh, Ultimate strength of continuous composite beams in combined bending and shear, J. Constr. Steel Res. 60 (8) (2004) 1109–1128.

[22] Q.Q. Liang, B. Uy, M.A. Bradford, H.R. Ronagh, Strength analysis of steel–concretecomposite beams in combined bending and shear, J. Struct. Eng. ASCE 131 (10)(2005) 1160–1593.

[23] Lasheen, Mahmoud, Amr Shaat, and Ayman Khalil. "Numerical evaluation for the effective slab width of steel-concrete composite beams." Journal of Constructional Steel Research 148 (2018): 124-137.